Environment and Ecology 42 (4) : 1615—1622, October—December 2024
Article DOI: https://doi.org/10.60151/envec/AHPY4988
ISSN 0970-0420

Influence of the Western Disturbance on Winter Precipitation: Observations Over the Central Himalayas using VHF Radar

Samaresh Bhattacharjee, Manish Naja, Kishan Singh Rawat, Vinod Kumar Tripathi

Received 19 July 2024, Accepted 1 September 2024, Published on 18 October 2024

ABSTRACT

This study investigates the influence of the Western Disturbance (WD) on atmospheric wind patterns and associated precipitation over the Himalayan region utilizing observations carried out using the ARIES ST Radar (ASTRAD) at Nainital [29.36° N, 79.46° E, 1800 m] during March 2024. The observations reveal that during the WD events, the wind direction was predominantly south westerly/westerly with varying speeds, reaching up to 67 m/s. The HYSPLIT model back-trajectory analysis confirmed that the moisture-laden air masses originated from the Atlantic Ocean. Vertical wind measurements indicated significant atmospheric instability and convection, characterized by updraft and downdraft motions in three distinct height regions between 8 km and 10 km, an updraft between 6 km and 7 km, and another downdraft between 4.5 km and 5 km. The core height region of the subtropical westerly jet (SWJ) embedded in WD and shift in height with maximum wind speed are also identified.

Keywords Western disturbance, VHF Radar, Himalayas, Rainfall, Crops, Convection.

Samaresh Bhattacharjee[1]
Engineer- 'F', Aryabhatta Research Institute of Observational Sciences (ARIES), Nainital, Uttarakhand

Present Affiliation: Graphic Era (Deemed to be University), Dehradun, Uttarakhand, India

Manish Naja[2]
Scientist-'G', Aryabhatta Research Institute of Observational Sciences (ARIES), Nainital, Uttarakhand

Kishan Singh Rawat[3]
Professor, Graphic Era (Deemed to be University), Dehradun, Uttarakhand, India

Vinod Kumar Tripathi[4*]
Associate Professor, Department of Agricultural Engineering, Institute of Agricultural Sciences, Banaras Hindu University, India

Email: vktripathi@bhu.ac.in
*Corresponding author

INTRODUCTION

Western Disturbance (WD) is a synoptic meteorological phenomenon that significantly affects the weather patterns in the Indian region. It originates from the Mediterranean region and progresses eastward due to westerly winds and troughs embedded within the subtropical westerly jet (SWJ). Along the progression, this westerly wind brings moisture, which results in rain and snowfall during Indian winter over Northern India, including the Himalayan regions (Hasan and Pattnaik 2023, Ranade *et al.* 2024). This winter rainfall and moisture influx with WD is necessary to produce winter crops (Hunt *et al.* 2024). Rainfall associated with WD is also essential for replenishing glaciers and sustaining the perennial rivers originating

from the Himalayas to ensure the availability of water resources throughout the year. Hence, the timely arrival of WD is essential in many ways to support agriculture, economy, and livelihood. However, excessive precipitation caused by WD can sometimes lead to crop damage, landslides, floods, and avalanches (Rangachary and Bandyopadhyay 1987).

Recently, a decreasing trend in the winter frequency of WD has been reported (Das *et al.* 2002 and Kumar *et al.* 2015). This decline in WD frequency has resulted in a decline in WD-associated rainfall over the core WD zone covering Jammu and Kashmir, Himachal Pradesh, and Uttarakhand in the Northern part of India (Javed *et al.* 2023). This change in the dynamics of WD is directly linked to regional climate change (Dimri *et al.* 2015). The Northwest part of India has recently witnessed a dry spell in winter with significantly low snow and rainfall.

According to the India Meteorological Department (IMD) annual report 2023 (https://mausamjournal.imd.gov.in/index.php/MAUSAM/Annualreport), the state of Uttarakhand has witnessed a 59% deficiency in total rainfall in the post-monsoon period. Another report from IMD dated 18 January 2024 (https://internal.imd.gov.in/pages/press_release_mausam.php) says that there was a 96% deficiency in winter rainfall in the Northwest part of India during the first half of January 2024. Hence, understanding the dynamics of WD with particular attention to the Himalayan region is required, where observation data collection is limited due to its challenging terrain. In this direction, a case study of WD during the first week of March 2024 from Nainital, Uttarakhand, is presented. The WD episode continued for about three days with moderate rainfall.

The paper is organized in the following way. Section 2 describes the observation site and methodology. Results and discussion are presented in section 3, and section 4 describes the conclusion.

MATERIALS AND METHODS

Observation site and methodology

The observation was from Aryabhatta Research Institute of Observational Sciences (ARIES) (29.36° N, 79.46° E, 1800 m) Nainital, Uttarakhand. The location of ARIES is marked in Fig. 1(a). Nainital is located northwest of the central Himalayan region and close to the mean position of the primary SWJ over India at 31^0 N (Singh 1971). Under the influence of WD, the site occasionally experiences heavy to extreme rainfall and snowfall during winter and the post-monsoon period (Rawat *et al*. 2022). Hence, the site is ideally suited for studying WD and its effects on the Himalayan region.

Winter precipitation is most active between November and March (Raghavan *et al.* 2019). Hence, to select dates for the case study, the rainfall data for six

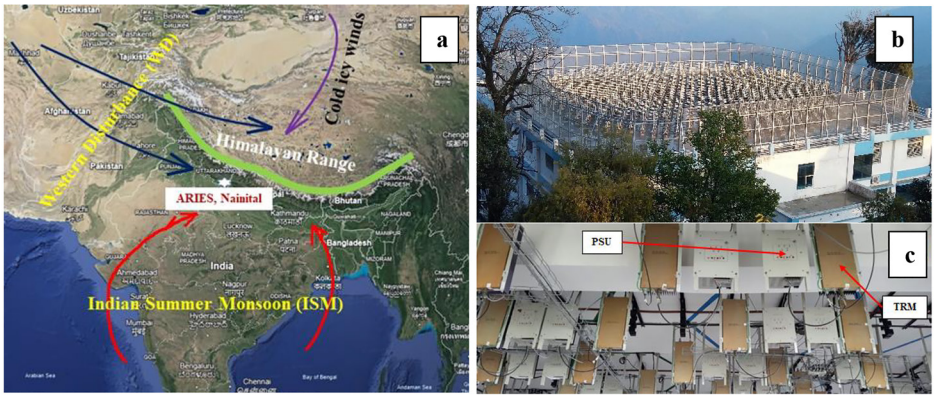

Fig. 1. (a) The location of ARIES, Nainital, (b) Antenna array of ARIES ST Radar (ASTRAD) on the roof top of the building and (c) Network of TRM below the rooftop.

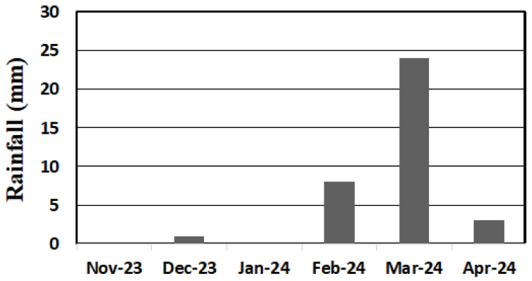

Fig. 2. The monthly rainfall data from November 2023 to April 2024 recorded from ARIES, Nainital.

months from November 2023 to March 2024, after monsoon and during winter, recorded in Automatic Weather Station (AWS) from the site, is analyzed (Fig. 2). It illustrates that the site experienced almost negligible rainfall from November to January 2024. In the next three months, it gradually reached a maximum in March 2024 and decreased again by April 2024. This maximum rainfall in March 2024 draws attention to observing the wind pattern to understand the influence of WD behind it.

The pattern of atmospheric wind has been obtained from ARIES ST Radar (ASTRAD). It is an active aperture radar system comprised of a network of antenna and Transmit Receive Module (TRM) with Power Supply Unit (PSU) shown in Figs. 1(b-c). The ASTRAD follows the basic operational principle of a pulsed Doppler radar and operates at 206.5 MHz. The radar's operating frequency is sensitive to both backscattered signals from clear air turbulence eddies and hydrometeors. ASTRAD employs the Doppler Beam Swinging (DBS) technique to estimate zonal (U), meridional (V), and vertical (W) wind in the atmosphere. This technique involves five beams: One towards the zenith and four in off-zenith directions. The off-zenith beams oriented towards the North and South directions estimate the meridional component, while the zonal component is calculated from the beams directed towards the East and West. The zenith beam allows for the direct estimation of the vertical component. This component is crucial in understanding deep convection and various types of rainfall (Callaghan and Power 2017). Processing the Doppler-shifted backscattered signal from eddies

Table 1. The values of parameters set in ESF for the ASTRAD operation.

Sl. No.	Parameters	Value
1	No. of FFT points (NFFT)	512
2	No. of coherent integration (NCOH)	96
3	Pulse width (PWD in μs)	16
4	Coded baud length (CBL)	0.5 μs
5	No. of Incoherent integration (NICOH)	4
6	Inter pulse period (IPP in μs)	200
7	Off-zenith scanning angle (degree)	15
8	No. of beams	5 (North, South, Zenith, East and West)
9	No. of range bin for height	240

carried by background wind, ASTRAD produces the height profile of the atmospheric wind. This profile is further used to understand atmospheric circulation and dynamics. More about the ASTRAD system can be found in Bhattacharjee *et al.* (2022). The parameters of ASTRAD in Experimental Specification Files (ESF) set for the radar observations to obtain the atmospheric wind for the present studies are displayed in Table 1.

In the ESF, the pulse width and IPP combination were adjusted to radiate sufficient pulsed electromagnetic energy and cover the maximum possible height simultaneously. The 0.5 μs CBL allows to achieve fine height resolution as low as 75. This 75 m height resolution with 240 range bins in 200 μs IPP achieved a maximum height coverage of 21 km from amsl. Coherent and incoherent integration improved the signal-to-noise ratio in the time and frequency domains, respectively.

In addition to the radar observations, back-air trajectory simulations are made using the HYSPLIT trajectory model, and ECMWF-Reanalysis-5 (ERA-5) reanalysis data (0.25° × 0.25°) are also used for winds. The HYSPLIT by NOAA's Air Resources Laboratory is a numerical model for computing air mass trajectories and is widely used for back-trajectory analysis, determining air mass origins, and assessing source–receptor relationships (Stein *et al.* 2016).

The data of ASTRAD is analyzed by the ASTRAD data processing Tool (ADPT), and more about

the ADPT is available can be found in Bhattacharjee *et al.* (2022). Heights in all plots are shown from above mean sea level (amsl), and the starting height is decided by the first data captured by the radar as per set PWD.

RESULTS AND DISCUSSION

This section discusses the results after observation and analysis of data obtained from ARIES ST Radar and models.

Atmospheric wind observations

The observation of atmospheric wind using ASTRAD over a total of 9 days (from 26 February to 27 February 2024 and from 1 March to 7 March 2024) is shown in Fig. 3(a).

The radar was operated with the parameters of the ESF file mentioned in Table 1. The figure only includes the wind profiles displaying the maximum wind speeds during the observation period. Alongside the wind plot, rainfall data for 11 days from 26 February to 7 March 2024 is depicted in Fig. 3(b). The total rainfall recorded in March 2024, 24 mm, occurred over three consecutive days from 2 March to 4 March 2024, with 5 mm, 10 mm, and 9 mm, respectively. Figure 3(a) illustrates that the maximum wind speed gradually increased from 46 m/s on 26 February 2024 to 64 m/s on 4 March 2024. After the episode, the wind speed increased slightly, reaching a maximum of 67 m/s on 6 March 2024. The figure also shows a significant change in the height region with maximum speed from 1 March to 3 March 2024, marked with a dotted line. The maximum wind speed was around 52 m/s at a height of 12.68 km on 1 March 2024. The next day, on 2 March 2024, the maximum wind speed was 59 m/s at a height of about 16.5 km. The position of the maximum wind speed of 63 m/s descended to 13.5 km on 3 March 2024. On 4 March 2024, the maximum wind speed region further descended to around 12.98 km with a speed of 64 m/s. Thus, the height of the maximum wind speed region ascended by about 3.82 km from 1 March to 2 March 2024 and descended by about 3.5 km from 2 March to 4 March 2024. This change in height coincides with the rainfall episode when the average maximum wind speed was 63 m/s (or about 227 km/h), and the mean position of the maximum wind speed region was at a height of about 14.3 km amsl (Fig. 3).

The detailed wind pattern from 2 March to 4 March 2024 during the rainfall days is shown in Fig. 4. To capture the wind pattern, the radar was operated for three hours (16 hours to 19 hours) on 2 March 2024, eight and half hours (930 hours to 18 hours) on 3 March 2024, and three and half hours (930 hours to 1730 hours) on 4 March 2024 with no observation from 12 hours to 16.5 hours. The data from the said operation hours was analyzed to derive the wind speed and direction displayed in Fig. 4. It illustrates that during the days of rainfall, the wind direction over the site remained south westerly/westerly throughout

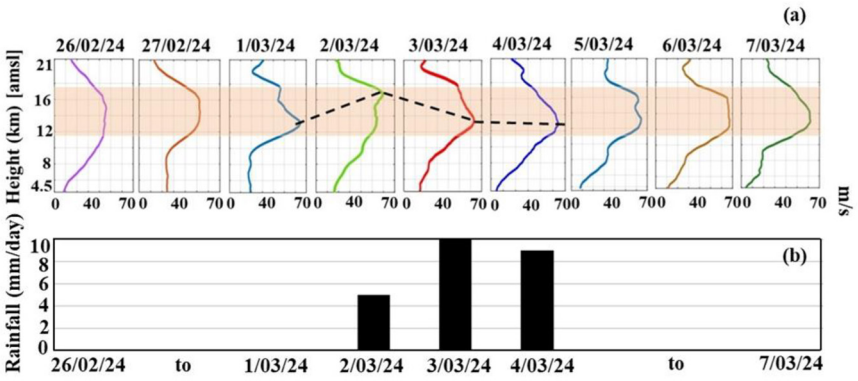

Fig. 3. (a) The wind speed of a single profile from 26 February 2024 to 7 March 2024. The shift in the height of maximum wind speed from 1 March to 4 March is marked as dotted line, (b) Rainfall data recorded from 26 February to 7 March 2024.

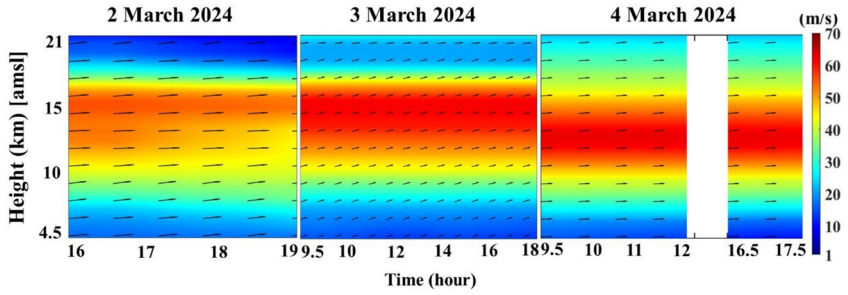

Fig. 4. The wind speed and direction for the observation period on 2 March, 3 March, and 4 March 2024.

the height range from 4.5 km to 21 km. and the wind speed varied with height. It initially increased from around 20 m/s, reaching a maximum between the 12 km and 16.5 km height regions. Then, the wind speed gradually decreased to below 10 m/s at a height of 21 km. The shifts in the region with maximum wind speed between 1 March and 4 March 2024 (Fig. 3 (a)) are further investigated by the gross features from the available observation of ASTRAD and comparison made with ERA5 data (Fig. 5). The figure shows the overall features of the WD from 10 hours on 1 March 2024 to 17 hours on 4 March 2024. The radar was operated for eight hours and thirty minutes (10 to 1830 hours) on 1 March 2024. To get the gross features from ASTRAD, the data gap was averaged. In the case of ERA5, data resolution is one hour.

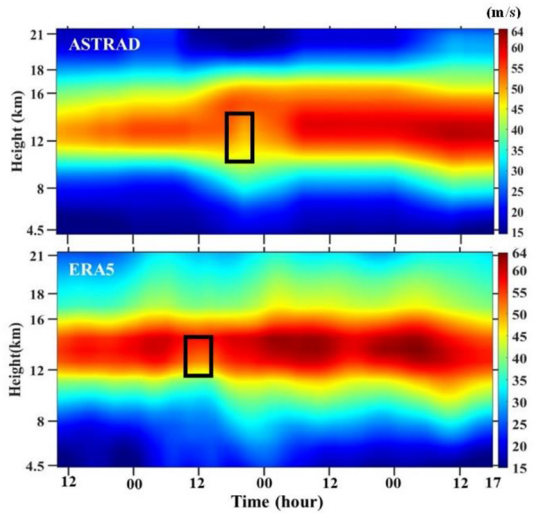

Fig. 5. Time and height variation of wind speed from 1 March 2024 to 10 hours to 4 March 2024, 17 hours showing position SWJ (up) from ASTRAD, (down) ERA5.

The gross features, including the features of the core region, which has considerable wind speed (> 50 m/s) embedded in it, are reasonably matched from ASTRAD and ERA5. ASTRAD observations indicate that the height spread of the core region gradually increased from ~ 2 km at 10 hours on 1 March 2024 to ~ 5 km at 12 hours on 2 March 2024, ERA5 also shows a similar trend but with a comparatively slow increase in width of the core region and wider spread in height ~ 4 -5 km.

Both plots demonstrate that the core region was widened further on 3 March 2024, with a maximum wind speed of 64 m/s. On 4 March 2024, the top height region of the SWJ descended, which is reflected in both plots. The shift in the height with maximum wind speed on 2 March 2024, as shown in Fig. 3, is marked with a black box on the wind speed plot from the ASTRAD. A similar feature in wind speed from ERA5 on 2 March 2024 is also marked with another black box. In ERA5, the shift event occurred around 12 hours, approximately 6 hours before a similar shift event observed in ASTRAD observations, which occurred around 18 hours.

Back trajectory from HYSPLIT model

The atmospheric wind observation from ASTRAD revealed that during the rainfall days over the site, wind flowed from the west/southwest with speeds as high as 230 km/h (64 m/s). The direction, speed, and height region where this high wind was observed

indicate a strong presence of a WD. As WD is a synoptic-scale weather phenomenon, the HYSPLIT model was simulated for 72 hours back trajectory to understand the origin of the air masses (Fig 6). The wind speed observation shows (Figs. 3-4) that the considerable wind speed lies within the height region between 10 km and 16.5 km. Hence, the model for back trajectory ran at 10,000 m, 14,000 m, and 16,000 m heights starting from 4 March 2024. At each height, 24 back trajectories were generated at intervals of 4 hours. The Relative Humidity (RH) level is also depicted along the trajectory.

The back trajectory analysis shows that the westerly air masses originated from the Atlantic Ocean and crossed the Mediterranean and the Arabian Sea during the period. After traversing these major water bodies, air masses eventually reached the study area. The influx of moisture-laden air encountered the complex topography of the Himalayas over the observation site, and subsequent rainfall occurred during the period.

Winter convection process

Over the Himalayan topography, WD is sometimes associated with an orography-induced convection process and rainfall (Hasan and Pattnaik 2023). A convection process can be characterized by updraft and downdraft motion in vertical wind simultaneously in the atmosphere. The zenith beam observations from ASTRAD on the highest rainfall day, 3 March 2024, are utilized to measure the vertical component

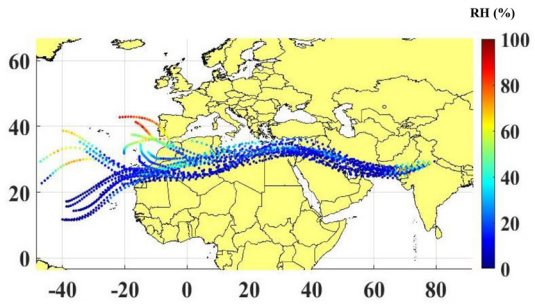

Fig. 6. 72 hours back trajectory starting from 4 March. The RH level along the trajectory is also shown.

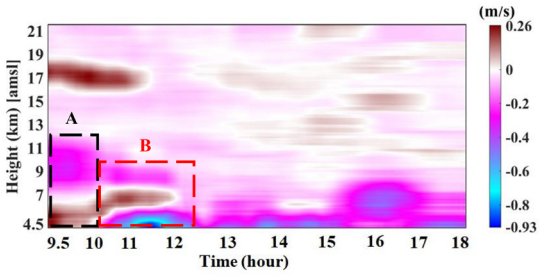

Fig. 7. Observation of vertical wind on 3 March 2024.

of atmospheric wind, thereby aiding in understanding the convective processes in the atmosphere (Fig. 7). It illustrates that during the entire observation period from 9.5 hours to 18 hours on 3 March 2024, the lower atmosphere below 11 km was more unstable with vertical downdraft and updraft motion. In that period, instabilities in zone 'A' (marked as a black dotted box) and zone 'B' (marked as a red dotted box) were identified as times when the atmosphere was more convective, with strong updraft and downdraft motion, accompanied by changes in height. In the zone 'A,' between 9.5 hours and 10 hours, an updraft up to the height of 6.5 km with a maximum wind speed of 0.26 m/s and a downdraft from 7 km to 12 km with a speed of approximately 0.2 m/s were recorded. Zone 'B' was more violent, with three height zones characterized by vertical wind direction changes: A downdraft between 8 km and 10 km, an updraft between 6 km and 7 km, and another downdraft between 4.5 km and 5 km. Above zone 'A' and 'B,' between 17-19 km, a region of updraft with a maximum updraft speed of 0.26 m/s was also observed. These changes in wind direction signified more mixing of atmospheric layers. The presence of strong downdraft as high as 0.5 m/s was also observed from 12 hours to 18 hours. These observed instabilities reflect dynamic atmospheric conditions, significantly influencing the weather and precipitation during the WD episode.

CONCLUSION

The remote sensing study of Western Disturbance episodes over the central Himalayan region using the ARIES ST Radar (ASTRAD) is discussed. The wind speed profiles from 26 February 2024 to 7 March

2024 reveal significant insights into the behavior of wind patterns and their impact on local weather. The ASTRAD observations indicate a consistent increase in wind speed, peaking between 3 March and 4 March 2024, which coincided with the rainfall episode over the observation site. The observed wind direction remained predominantly south westerly/westerly throughout the height range of 4.5 km to 21 km, with maximum wind speeds reaching up to 67 m/s. The back trajectory analysis from the HYSPLIT model highlighted the origins of the westerly air masses, tracing their path from the Atlantic Ocean across the Mediterranean and the Arabian Sea before reaching the study area. Additionally, the vertical wind observations on 3 March 2024 showcased the dynamic nature of the lower atmosphere, with notable updrafts and downdrafts indicating significant convective activity. During the observation period, updrafts up to 0.26 m/s and downdrafts up to 0.5 m/s were recorded, reflecting the dynamic atmospheric conditions. ASTRAD observation reveals a gradual increase of the height spread of the core region with considerable wind speed (>50 m/s) from 1 March to 2 March 2024 between heights of 11-16 km from amsl. ASTRAD and ERA5 both datasets indicate a wider SWJ region on 3 March 2024, with max wind speeds of 64 m/s; the observations from ASTRAD suggest that there was an event of a shift in the height of maximum wind speed, which occurred approximately 6 hours later than a similar event indicated in ERA5. This study would help to enhance understanding of the general characteristics of Western Disturbances over the central Himalayan topography and their impact on rainfall during the non-monsoon period. The findings will offer valuable insights for future meteorological research and weather forecasting, which are crucial for the thriving of local flora and fauna.

ACKNOWLEDGMENT

We sincerely thank the Director, ARIES, for supporting and encouraging this work. We also thank Mr. Arjuna Reddy and Mr. Uday Singh for the radar observations. We acknowledge ECMWF for the ERA-5 reanalysis data, available at https://cds.climate.copernicus.eu/.

REFERENCES

Bhattacharjee S, Naja M, Jaiswal A, Rawat KS, Sagar R, Ananthakrishnan S (2022) *Journal of Astronomical Instrumentation,* 11(4): 2240005. World Scientific Publishing Company, https://doi.org/10.1142/S2251171722400050.

Callaghan Jeff , Power Scott. (2017) A vertical wind structure that leads to extreme rainfall and major flooding in southeast Australia. *Journal of Southern Hemisphere Earth System Science* 66 : 380-401. https://doi.org/10.22499/3.6604.002.

Das MR, Mukhopadhyay RK, Dandekar MM, Kshirsagar SR (2002) Pre-monsoon western disturbances in relation to monsoon rainfall, its advancement over NW India and their trends. *Current Science* 82 : 1320-1321.

Dimri AP, Niyogi Dev, Barros Ana, Ridley Jef, Mohanty UC, Yasunari Tetsuzo, Sikka D (2015) Western disturbances: A review. *Reviews of Geophysics* 53 : In prees https://doi.org/10.1002/2014RG000460.

Hasan Mirza, Pattnaik Sandeep (2023) Characteristics of Western Disturbance intensification and associated induced circulations over the Indian Region. Natural Hazards Research https://doi.org/10.1016/j.nhres.2023.12.002

Hunt Kieran, Baudouin Jean-Philippe, Turner Andrew, Dimri AP, Jeelani Gh, Pooja Pooja, Chattopadhyay R, Cannon Forest, Thanigachalam Arulalan, Shekhar M, Sabin TP, Palazzi Eliza (2024) Western disturbances and climate variability: A review of recent developments. 10.5194/egusphere-2024-820.

Javed Aaquib, Anshuman Katyan, Kumar Pankaj, Sachan Disha (2023) The decline in western disturbance activity over Northern India in recent decades. Climatic Change pp 176. https://doi.org/10.1007/s10584-023-03571-8.

Kumar Naresh, Yadav Payal, Gahlot Shilpa, Singh Manmohan (2015) Winter frequency of western disturbances and precipitation indices over Himachal Pradesh, India: *Atmósfera.* 95 : 1977-Sept. https://doi.org/10.1016/S0187-6236(15)72160-0.

Raghavan Krishnan, Sabin TP, Ranade Madhura, Vellore Ramesh, Mujumdar Milind, Sanjay J, Nayak Shailesh, Rajeevan M (2019) Non-monsoonal precipitation response over the Western Himalayas to climate change. Climate Dynamics pp 52. https://doi.org/10.1007/s00382-018-4357-2.

Ranade Madhura, Raghavan Krishnan, Revadekar Jayashree, Mujumdar Milind, Goswami BN (2014) Changes in Western Disturbances over the western Himalayas in a warming environment. Climate Dynamics, pp 44. https://doi.org/10.1007/s00382-014-2166-9.

Rangachary N, Bandyopadhyay B (1987) An analysis of the synoptic weather pattern associated with extensive avalanching in Western Himalaya. IAHS Publ, 162.

Rawat Kishan, Sahu Smruti, Singh Sudhir, Mishra Anil Kumar (2022) Cloudburst analysis in the Nainital district, Himalayan Region, 2021. *Discover Water* (2)12 : In prees. https://doi.org/10.1007/s43832-022-00020-y.

Singh MS (1971) The study of the jet stream over India and to its north in winter, Part-I. *Indian Journal of Hydrology & Geophysics* 22: 1-14. 10.54302/mausam.v22i1.3978.

Stein Ariel, Draxler RR, Rolph Glenn, Stunder Barbara, Cohen-Mark, Ngan F (2016) NOAA's HYSPLIT atmospheric transport and dispersion modeling system. *Bulletin of the American Meteorological Society.* 96 : 150504130527006. https://doi.org/10.1175/BAMS-D-14-00110.1.